Green Chemistry

Cutting-edge research for a greener sustainable future

www.rsc.org/greenchem

Volume 12 | Number 11 | November 2010 | Pages 1873–2068

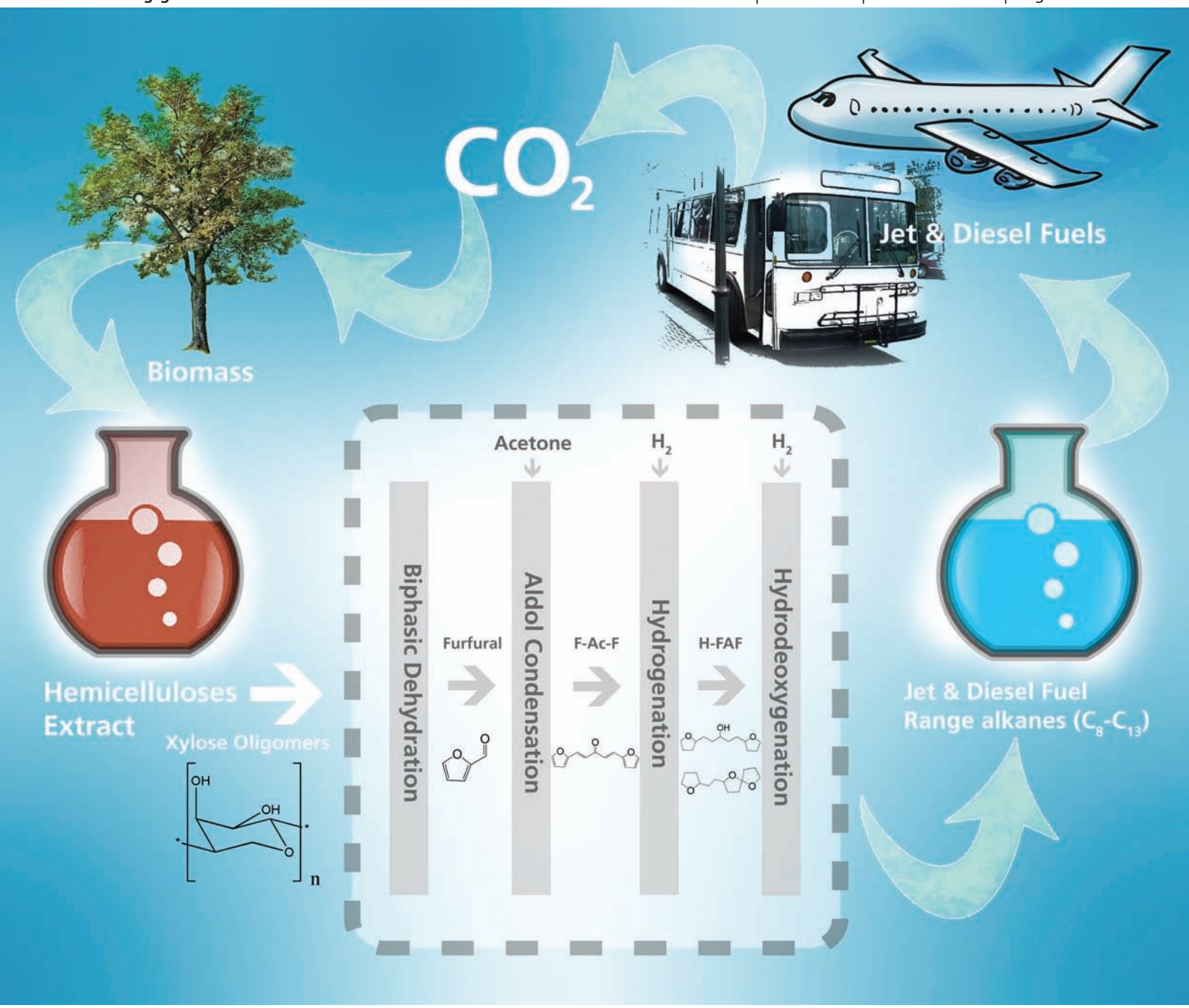

ISSN 1463-9262

RSC Publishing

COVER ARTICLE

Huber *et al.*

Production of jet and diesel fuel range alkanes from waste hemicellulose-derived aqueous solutions.

1463-9262(2010)12:11;1-C

Production of jet and diesel fuel range alkanes from waste hemicellulose-derived aqueous solutions†

Rong Xing,[a] Ayyagari V. Subrahmanyam,[a] Hakan Olcay,[a] Wei Qi,[a] G. Peter van Walsum,[b] Hemant Pendse[b] and George W. Huber*[a]

Received 25th June 2010, Accepted 27th August 2010
DOI: 10.1039/c0gc00263a

In this paper we report a novel four-step process for the production of jet and diesel fuel range alkanes from hemicellulose extracts derived from northeastern hardwood trees. The extract is representative of a byproduct that could be produced by wood-processing industries such as biomass boilers or pulp mills in the northeastern U.S. The hemicellulose extract tested in this study contained mainly xylose oligomers (21.2 g/l xylose after the acid hydrolysis) as well as 0.31 g/l glucose, 0.91 g/l arabinose, 0.2 g/l lactic acid, 2.39 g/l acetic acid, 0.31 g/l formic acid, and other minor products. The first step in this process is an acid-catalyzed biphasic dehydration to produce furfural in yields up to 87%. The furfural is extracted from the aqueous solution into a tetrahydrofuran (THF) phase which is then fed into an aldol condensation step. The furfural-acetone-furfural (F-Ac-F) dimer is produced in this step by reaction of furfural with acetone in yields up to 96% for the F-Ac-F dimer. The F-Ac-F dimer is then subject to a low-temperature hydrogenation to form the hydrogenated dimer (H-FAF) at 110–130 °C and 800 psig with a 5 wt% Ru/C catalyst. Finally the H-FAF undergoes hydrodeoxygenation to make jet and diesel fuel range alkanes, primarily C_{13} and C_{12}, in yields up to 91%. The theoretical yield for this process is 0.61 kg of alkane per kg of dry xylose derived from the hemicellulose extract. Experimentally we were able to obtain 76% of the theoretical yield for the overall process. We estimate that jet and diesel fuel range alkanes can be produced from between $2.06/gal to $4.39/gal depending on the feed xylose concentration, the size of the biorefinery, and the overall yield. Sensitivity analysis shows that the prices of raw materials, the organic-to-aqueous mass ratio in the biphasic dehydration, and the feed xylose concentration in the hemicellulose extract significantly affect the product cost.

1. Introduction

Diminishing fossil resources and growing environmental concerns increase the need to develop alternative renewable sources and technologies for the production of fuels and chemicals.[1,2] Jet and diesel fuels, as important liquid transportation fuels, are essential for modern economies. They are currently primarily produced from petroleum-based crude oils. Increasing demand for transportation fuels requires the sustainable production of jet and diesel fuels. This can be accomplished using non-food lignocellulosic biomass as a feedstock.[2,3] Lignocellulosic biomass and its derivatives have been processed in diverse ways to make hydrogen,[2,4–6] chemical intermediates,[7,8] and liquid hydrocarbon fuels including bio-oils,[9] aromatic hydrocarbons,[10–11] and bioethanols.[12–15,16] Vegetable oils can also be hydro-treated to produce straight-chain alkanes that can fit in the jet and diesel fuels range.[17] We have also used aqueous-phase hydrodeoxygenation to make gasoline range alkanes from both carbohydrates and bio-oils.[4,5,18] However, these lighter alkanes are not suitable to serve as jet and diesel fuel components due to their high volatility. Jet fuels are a complex hydrocarbon mixture consisting of different classes such as paraffin, naphthene, and aromatics. The range of their sizes (carbon numbers or molecular weights) is restricted by the requirement for the product, for example, the distillation profile, the freezing point or smoke point.[19] Currently, Jet-A and JP-8 are used to power civilian and military aircrafts. Typically JP-8 consists of n-paraffin ranging from C_8–C_{15} (~35 wt%), branched paraffin ranging from C_8–C_{15} (~35 wt%), aromatics ranging from C_7–C_{10} (18 wt%) and cycloparaffin ranging from C_6–C_{10} (7 wt%).[20]

Huber *et al.*[21] first presented a catalytic process for the conversion of biomass-derived carbohydrates to liquid alkanes (C_7–C_{15}) that serve as jet and diesel fuel components in a four-phase reactor system. In the Huber *et al.* work they used model compounds for this process. The first step in this process is a dehydration step to produce furfural from C_5 sugars and 5-hydroxylmethylfurfural (HMF) from C_6 sugars. Dumesic and co-workers later developed a highly efficient biphasic process that was able to produce HMF and furfural

[a]*Department of Chemical Engineering, University of Massachusetts, Amherst, 686 North Pleasant Street, 159 Goessmann Lab, Amherst, MA, 01003, USA. E-mail: huber@ecs.umass.edu; Fax: +1 413-545-1647; Tel: +1 413-545-0276*
[b]*Chemical and Biological Engineering Department, Forest Bioproducts Research Institute (FBRI), University of Maine, 5737 Jenness Hall, Orono, ME, 04469-5737, USA.*
† Electronic supplementary information (ESI) available: Tables S1 and S2. See DOI: 10.1039/c0gc00263a

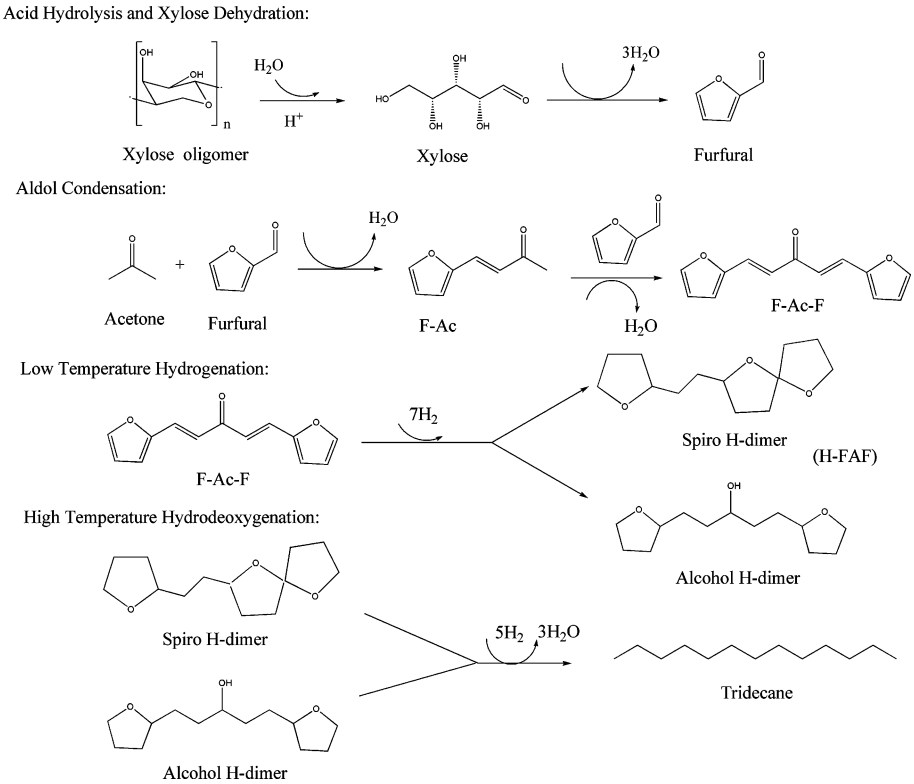

Fig. 1 Reaction chemistry for the conversion of xylose oligomers into tridecane.

in high yields.[1,22] The furfural and HMF are then reacted with acetone by a base-catalyzed aldol condensation step to produce alkane precursors, *e.g.*, monomers and dimers. These monomers and dimers are then converted into straight-chain alkanes by a dehydration/hydrogenation step. While this initial process looks promising for the production of large straight alkanes for jet and diesel fuels, to date researchers have only used model biomass compounds that do not contain the impurities present in biomass feedstocks. In this paper we use aqueous carbohydrate solutions derived from northeastern hardwood trees. Aqueous carbohydrate feedstocks could be produced as a by-product stream by wood-processing industries that obtain relatively low value from hemicelluloses.[16,23,24] The extract used in this study was derived through hot-water extraction and is representative of a process stream that could be produced at a biomass power plant or composite wood manufacturing facility. The four steps to make jet and diesel fuel range alkanes require process integration and optimization. In this paper we show how this process could be integrated, and also perform an economic analysis.

As of today, there has been no report on the direct use of lignocellulosic hydrolysates for the production of diesel and jet fuel range alkanes. The objective of this paper is to report on a novel integrated four-step process by which jet and diesel fuel range alkanes (C_8–C_{13}) can be produced from hemicellulose-derived aqueous solutions and show that high yields of alkanes can be achieved under optimized conditions. Fig. 1 depicts the key reaction chemistry involved in the production of tridecane from the hemicellulose extract. This process includes four steps: (1) acid hydrolysis and xylose dehydration, (2) aldol condensation, (3) low-temperature hydrogenation, and (4) high-temperature hydrodeoxygenation.

The hemicellulose extract we used in this work was produced by extracting wood chips with hot water in a custom-built rotating digester at the University of Maine Process Development Center.[24] The first step in our process is a combined acid hydrolysis of xylose oligomers and biphasic dehydration of xylose. The hemicellulose extract contains monomeric xylose and xylose oligomers (~1.3 g/l xylose monomer and ~19.9 g/l xylose oligomers). The xylose oligomers are first converted into monomeric xylose through the acid-catalyzed hydrolysis.[25] The xylose monomers are then converted into furfural and water through the acid-catalyzed dehydration. The dehydration of pure xylose into furfural has been studied in monophasic,[26] biphasic (organic and aqueous phase, single solvent and solid acids)[22,27,28] and triphasic reaction systems (organic, aqueous phase and solid acids),[27,29] using catalysts such as mineral acids,[22,26,28] solid acids.[27,30] Among them, the reaction systems consisting of both organic and aqueous phase showed a simultaneously high xylose conversion and a high selectivity for furfural. Dias and coworkers reported that 91% conversion of xylose and 83% selectivity of furfural could be achieved by using toluene–water as solvent over a micro-mesoporous sulfonic acid catalysts.[27] Dumesic and co-workers obtained 71% conversion of xylose and 91% selectivity of furfural using 7 : 3 (w/w) methyl isobutyl ketone (MIBK)–2-butanol as solvent with HCl as a catalyst.[22] In the biphasic systems, the organic solvent is usually used as an extracting solvent that extracts furfural from the aqueous phase to avoid undesired decomposition reactions of furfural which produce formic acid,[31] and solid humins.[32] In

Table 1 Chemical compositions of the un-hydrolyzed and hydrolyzed hemicellulose extract (H-extract) used in this study

	Concentration (g/l)									
H-extract	Glucose	Xylose	Arabinose	Lactic Acid	Formic Acid	Acetic Acid	HMF	Furfural	TOC (ppm)	% Carbon Identified
Un-hydrolyzed	0.31	1.31	0.91	0.20	0.31	2.39	0.05	0.12	24 285.6	9.0
Hydrolyzed	0.79	21.2	1.1	0.12	0.32	4.77	0.041	0.553		47.8

the present work, THF was selected as the extracting solvent due to its great affinity for furfural, low boiling-point (66 °C), low vaporization heat (30 kJ/mol), and ease of separation from water. The addition of simple salts to the aqueous phase was found to improve the separation of organic and aqueous phases due to the "salting-out" effect.[1] We added NaCl into the hemicellulose extract in order to enhance the partitioning of furfural into the organic phase.

In the second step, furfural reacts with acetone to form precursors of jet and diesel fuel range alkanes *via* the base-catalyzed aldol condensation. Aldol condensation occurs between two carbonyl groups (with at least one reactive α-hydrogen in either carbonyl group) over an acid or base catalyst, to form a β-hydroxycarbonyl derivative followed by a dehydration to produce α,β-unsaturated carbonyl compounds.[33–34] Accordingly, aldol condensation of equal molar amounts of furfural and acetone makes F-Ac monomer (C_8 species), while 2 moles of furfural with 1 mole of acetone produce F-Ac-F dimer (C_{13} species), as illustrated in Fig. 1. In this work the reaction was optimized to make high yields of F-Ac-F dimer.

The third step in our process is low-temperature hydrogenation. The purpose of this step is to stabilize the F-Ac-F dimer by producing hydrogenated F-Ac-F (H-FAF, spiro H-dimer or alcohol H-dimer in Fig. 1). F-Ac-F is unstable and will polymerize even at room temperature due to the presence of various unsaturated bonds. This step also helps avoid undesired plugging of reactors used in the subsequent hydrodeoxygenation step. In our work, the 5 wt% Ru/C powder catalyst was used due to its high reactivity and high efficiency of hydrogenating the double bonds.[5]

The hydrogenated dimers then undergo the last step of hydrodeoxygenation to produce tridecane. In our work, a 4 wt% Pt/SiO_2–Al_2O_3 catalyst was used due to its bi-functional properties.[4–5,35] The acidic SiO_2–Al_2O_3 catalyzes the dehydration of H-dimers to form C=C bonds and water, and the C=C bonds are hydrogenated over Pt.

The overall stoichiometric reaction for these four steps can be written as:

$$\begin{aligned} &2C_5H_{10}O_5 + C_3H_6O + 12H_2 \rightarrow C_{13}H_{28} + 11H_2O \\ &\frac{75}{46}\text{kg } C_5H_{10}O_5 + \frac{29}{92}\text{kg } C_3H_6O + \frac{3}{23}\text{kg } H_2 \rightarrow \\ &1\text{kg } C_{13}H_{28} + \frac{99}{92}\text{kg } H_2O \end{aligned} \quad (1)$$

Theoretically, 1.0 kg of tridecane can be produced from the following raw materials: 1.6 kg xylose (or xylose oligomers), 0.3 kg of acetone and 0.13 kg of H_2

2. Experimental and materials

2.1 Materials

Hemicellulose extract was obtained from the University of Maine. In their process mixed hardwood chips comprised primarily of maple (~50%) with lesser amounts of beech, birch and poplar, obtained from Red Shield Pulp & Chemicals (Old Town, ME, USA), were extracted with hot water in a custom-built rotating digester. Typically in each batch, 7 kg of wood (on an oven-dry basis) was added to the digester at a liquor-to-wood ratio of 4 : 1. The extraction was performed at a maximum temperature of 160 °C for a target H-factor of 360 h.[24] Table 1 shows the chemical compositions of the hydrolyzed and un-hydrolyzed hemicellulose extract. The hemicellulose extract was hydrolyzed at pH 1.0 with sulfuric acid at 130 °C for 30 min in an autoclave.[24] The feed used for our study was un-hydrolyzed and the xylose was primarily in the form of oligomers. Tetrahydrofuran (THF, 99+%), acetone (histological grade), NaOH (granular), NaCl (granular), HCl (37 wt%) were all purchased from Fisher Scientific and used as received.

2.2 Experimental and analysis

2.2.1 Acid hydrolysis and xylose dehydration. The combined acid hydrolysis of xylose oligomers and xylose dehydration were conducted in a biphasic batch reactor of 120 ml or 160 ml. The required amount of NaCl was first added into the sugar solution at room temperature to saturate the aqueous phase. The resulting sugar solution and THF were then mixed together in the reactor, followed by the addition of the required amount of HCl. The reactor was purged several times with helium to remove air and charged to 220 psig helium pressure. The reactor was then heated to 160 °C with vigorous stirring and held for different times ranging from 5 to 60 min. Finally, the reactor was immediately quenched in an ice bath to stop the reaction. The products were analyzed by using a Shimadzu high-performance liquid chromatograph (HPLC) equipped with both UV and RI detectors. Xylose content was detected with an RI detector (RID-10A, cell temperature 30 °C). Product of furfural was detected with a UV-vis detector (SPD-20A) at a wavelength of 254 nm. The column used was a Biorad© Aminex HPX-87H sugar column and the column oven temperature was held constant at 30 °C. Isocratic elution mode was used with the mobile phase of 0.005 M H_2SO_4 at a flow rate of 0.6 ml/min.

2.2.2 Aldol condensation. Aldol condensation of furfural with acetone was conducted at atmospheric pressure in a biphasic catalytic system consisting of a reactive aqueous phase and an organic extracting phase. The organic phase was created by adding acetone to the solution of furfural in THF produced

from the biphasic dehydration, and the aqueous phase consisted of 6.5–26 wt% NaOH and saturated NaCl (if used). In order to make F-Ac-F dimer, the molar ratio of furfural to acetone was kept constant as 2. The mixture was stirred vigorously at temperatures ranging from 25 °C to 80 °C for 24 h and the aldol adducts in THF were obtained through the liquid–liquid separation. The experiments were carried out in different reactor sizes ranging from 50 ml to 500 ml. The products of F-Ac-F and F-Ac were analyzed by using a HPLC with a SPD-20 AV UV (330 nm) detector, and a reverse-phase C-18 column from Agilent was used. Gradient elution mode was used with the mobile phase of a methanol–water mixture (volume ratio of methanol to water = 3 : 1) and pure methanol at a total flow rate of 0.8 ml/min.

2.2.3 Low-temperature hydrogenation. The effluent of the aldol reactor was subsequently hydrogenated in a batch reactor of 120 ml at 110–130 °C and 800 psig with a 5 wt% Ru/C powder catalyst (Strem Chemicals). Hydrogen was consumed during the reaction and more was supplied from time to time to maintain the pressure. The products were analyzed by a Shimadzu gas chromatograph (GC) (model 2010). A flame ionization detector (FID) was used to quantify the hydrogenation products. The GC–MS equipped with a Restek Rtx-VMS (Catalog No. 19915) column was used to identify the hydrogenation products. The hydrogenated products separated by a column chromatography and verified by using ^{1}H and ^{13}C NMR were used as standard compounds for calibration. For GC–MS, ultra-high purity helium was used as the carrier gas, and the temperatures of injector and detector were both set at 240 °C. The GC oven was programmed with a following sequence: hold at 35 °C for 5 min, ramp to 240 °C at 10 °C/min and hold at 240 °C for 5 min.

2.2.4 Hydrodeoxygenation. The hydrogenated dimer in THF was subject to the hydrodeoxygenation in a continuous plug flow bed reactor with a 4 wt% Pt/Al_2O_3–SiO_2 catalyst. The catalyst was prepared by using the incipient wetness method. The required amount of tetraamineplatinum(II) nitrate (Strem Chemicals) in deionized water was added dropwise to the silica-alumina powder (SiO_2-to-Al_2O_3 ratio = 4, Davison SIAL 3125) with continuous mixing. The as-made catalyst was first dried in an oven at 80 °C for 8 h, then calcined in air at a flow rate of 200 cm^3/min with the following temperature regime: room temperature to 260 °C for 3 h, hold at 260 °C for 2 h. The obtained catalyst was reduced in H_2 at a flow rate of 200 cm^3/min with the following temperature regime: room temperature to 450 °C at 50 °C/h, hold at 450 °C for 2 h. The gaseous products were analyzed by an online Shimadzu GC (model 2010) equipped with FID and TCD detectors, and the liquid products were analyzed by GC–MS. The C_1–C_6 alkanes in the gas product were quantified by using FID detector. The catalyst was packed in the $^1/_4''$ stainless steel tubing with glass wool on both sides. Feed of the hydrogenated dimer (H-FAF) was pumped to the reactor by using a JASCO PU980 HPLC pump and hydrogen was supplied from the bottom. The backpressure regulator was used to maintain the system at the desired pressures.

2.3 Calculations

In the biphasic dehydration step, xylose conversion and furfural selectivity were calculated as shown below. Assuming that the xylose solubility in THF is negligible, the xylose concentration (μmol/ml), [Xylose], represents the aqueous phase concentration.

$$\text{Conversion} = \frac{[\text{Xylose}]_{\text{feed}} V_{\text{feed}} - [\text{Xylose}]_{\text{aq.}} V_{\text{aq.}}}{[\text{Xylose}]_{\text{feed}} V_{\text{feed}}} \times 100\% \quad (2)$$

$$\text{Selectivity} = \frac{[\text{Furfural}]_{\text{aq.}} V_{\text{aq.}} + [\text{Furfural}]_{\text{org.}} V_{\text{org.}}}{[\text{Xylose}]_{\text{feed}} V_{\text{feed}} - [\text{Xylose}]_{\text{aq.}} V_{\text{aq.}}} \times 100\% \quad (3)$$

In the biphasic aldol condensation step, furfural conversion and F-Ac-F dimer selectivity were calculated as given below. Given the low solubtility of F-Ac-F in water (as shown in Table S1†[36–39]), the F-Ac-F dimer concentration (μmol/ml) represents the organic phase concentration.

$$\text{Conversion} = \frac{[\text{Furfural}]_{\text{feed}} V_{\text{feed}} - [\text{Furfural}]_{\text{org.}} V_{\text{org.}}}{[\text{Furfural}]_{\text{feed}} V_{\text{feed}}} \times 100\% \quad (4)$$

$$\text{Selectivity} = \frac{[\text{F-Ac-F}]_{\text{org.}} V_{\text{org.}}}{[\text{Furfural}]_{\text{feed}} V_{\text{feed}} - [\text{Furfural}]_{\text{org.}} V_{\text{org.}}} \times 100\% \quad (5)$$

In the low-temperature hydrogenation step, F-Ac-F dimer conversion and hydrogenated F-Ac-F (H-FAFs) selectivity were calculated as given below.

$$\text{Conversion} = \frac{[\text{F-Ac-F}]_{\text{feed}} V_{\text{feed}} - [\text{F-Ac-F}]_{\text{final}} V_{\text{final}}}{[\text{F-Ac-F}]_{\text{feed}} V_{\text{feed}}} \times 100\% \quad (6)$$

$$\text{Selectivity} = \frac{[\text{H-FAFs}]_{\text{final}} V_{\text{final}}}{[\text{F-Ac-F}]_{\text{feed}} V_{\text{feed}} - [\text{F-Ac-F}]_{\text{final}} V_{\text{final}}} \times 100\% \quad (7)$$

For the above three processes, V represents the corresponding phase volume (ml), and the reaction yield is defined as conversion × selectivity.

In the hydrodeoxygenation process, carbon alkane yield = (total moles of carbon atoms in alkane products)/(total moles of carbon atoms in the feed of H-dimer) × 100%.

3. Results

3.1 Acid hydrolysis and xylose dehydration

The combined acid hydrolysis of xylose oligomers and xylose dehydration were conducted at 160 °C and 220 psig in a biphasic reactor using water–THF as solvent with HCl as the catalyst. We saturated the hemicellulose extract with NaCl by adding 20 g NaCl to 100 g hemicellulose extract.[13] This saturation was done to decrease the solubility of THF in the aqueous stream. The results for dehydration of hemicellulose extract are summarized in Table 2. Initially, the molar ratio of HCl to xylose was varied (Table 2, Runs 1–4) to study the effect of HCl amount on furfural selectivity. These experiments were conducted for 60 min by keeping the mass ratio of organic to aqueous phase at 2 : 1. As can be seen, all xylose was almost completely converted after 60 min of reaction. The furfural selectivity increases from 12.6% to 80.7% as the HCl/xylose molar ratio increases from

Table 2 Furfural production by the biphasic dehydration of aqueous sugar solutions. Feeds for reactions were hemicellulose extract (H-extract) containing 2.1 wt% xylose and its oligomers, except Run 11 which was an aqueous solution containing 3.6 wt% pure xylose. Equal amount by weight of aqueous solution was used and the reaction was controlled at 160 °C with the use of THF as the organic solvent. The NaCl content was kept at 20 wt% (relative to the amount of hemicellulose extract) for Runs 1–10, and 35 wt% for Run 11, respectively

Run #	Batch size (ml)	Sugar solution	$M_{org.}/M_{aq.}$ [a]	HCl/xylose[b]	Reaction time (min)	Xylose conversion (%)	Furfural selectivity (%)	Furfural yield (%)
1	160	H-extract	2	0.8	60	99.4	12.7	12.6
2	160	H-extract	2	1.6	60	99.1	40.1	39.8
3	160	H-extract	2	2.4	60	99.4	81.4	80.7
4	160	H-extract	2	3.1	60	99.8	83.6	83.4
5	160	H-extract	0.67	2.4	60	99.3	60.0	59.6
6	160	H-extract	1	2.4	60	99.1	79.0	78.6
7	160	H-extract	3	2.4	60	99.0	82.5	81.7
8	120	H-extract	2	3.1	30	99.8	85.2	85.0
9	120	H-extract	2	3.1	5	99.8	86.9	86.7
10	120	H-extract	1.5	3.1	5	99.6	85.2	84.7
11	160	Xylose	2	0.6	60	99.6	90.4	90.0

[a] Mass ratio of organic phase to aqueous phase. [b] Molar ratio of HCl to xylose.

Table 3 Aldol condensation of furfural with acetone in a biphasic batch reactor. All runs were conducted for about 24 h at atmospheric pressure. The molar ratio of furfural to acetone was kept constant at 2

Run #	Batch size (ml)	NaCl (wt%)	Feed furfural (wt%)	$M_{org.}/M_{aq.}$ [a]	NaOH/furfural[b]	T (°C)	Furfural conversion (%)	F-Ac yield (%)	F-Ac-F yield (%)
1	50	35	13.0	1.0	2.3	25	100	3.1	93.5
2	50	35	13.0	1.0	2.3	50	100	2.2	72.2
3	50	35	13.0	1.0	2.3	80	100	1.8	69.8
4	100	—	25.2	6.0	0.13	25	100	16.0	61.8
5	100	35	25.2	3.0	0.13	25	100	23.9	52.9
6	100	—	26.5	6.2	0.48	25	100	3.4	92.2
7	100	35	26.5	3.1	0.48	25	100	9.2	85.7
8	200	—	23.9	6.4	0.43	25	100	4.5	85.1
9	200	—	36.8	5.1	0.37	25	100	0.002	96.2
10	500	—	36.8	5.1	0.37	25	100	0.04	90.9

[a] Mass ratio of organic to aqueous phase. The organic phase consists of furfural, THF and acetone, and the aqueous phase consists of water, NaOH and NaCl (if used). [b] Molar ratio of NaOH to furfural.

0.6 to 2.4. This suggests that high acid concentration is necessary to obtain high selectivity of furfural. Similar effects were reported using 5 : 5 (w/w) water–DMSO mixture and 7 : 3 (w/w) MIBK–2-butanol as the organic phase.[22] Further increasing the ratio of HCl to xylose to 3 : 1 improves the selectivity by only 3%.[27,32]

In pure water, the dehydration of xylose yields a low selectivity of only 47% due to the presence of side reactions including fragmentation, condensation, and resinification.[27] The addition of THF to the aqueous phase improves the selectivity for furfural by extracting out the furfural before it can undergo undesired reactions. The effect of the organic-to-aqueous mass ratio on the dehydration performance was investigated by keeping all other conditions constant as shown in Table 2 (Runs 2 and 5–7). As we can see from these runs, the furfural selectivity increased from 60% to 79% as the organic-to-aqueous mass ratio increased from 0.67 to 1. Further increasing the mass ratio to 3 : 1 caused a slight increase of furfural selectivity up to 81.7%. Runs 4 and 8–10 in Table 2 demonstrate the effect of reaction time on the xylose conversion, furfural selectivity and yield. A decrease of reaction time increases the furfural yield. For comparison, Run 11 shows the result of dehydration of pure xylose, and the 90% yield for furfural could be obtained even at a lower HCl/xylose ratio of 0.6. This suggests that a higher acid concentration is needed for furfural production from the hemicellulose extract than from pure xylose, possibly because high acid conditions are favorable for the hydrolysis of xylose oligomers to form xylose.

3.2 Aldol condensation

The results for aldol condensation of furfural with acetone in a batch reactor are summarized in Table 3. For all runs, the conversions of furfural were almost complete. The effect of temperature on the selectivity of the aldol products was studied using a 13 wt% furfural in THF with a stoichiometric amount of acetone (molar ratio of furfural to acetone = 2) added to the organic phase as shown in Runs 1–3 of Table 3. The reaction was conducted in the presence of saturated NaCl in a 50 ml reactor (NaOH: furfural molar ratio = 2.3 : 1, $M_{org.}$:$M_{aq.}$ = 1 : 1). The selectivity for both F-Ac and F-Ac-F decreases from 3.1% to 1.8% and from 93.5% to 69.8%, respectively, as the reaction temperature increases from 25 °C to 80 °C. However, the distribution of F-Ac and F-Ac-F products has little variation with temperature. The lower selectivity to F-Ac-F observed for higher reaction temperatures (50 °C and 80 °C) was probably caused by the degradation of F-Ac-F due to its thermally instability. Aldol condensation with and without adding NaCl into the reactive aqueous phase was performed

in a 100 ml biphasic reactor (Runs 4–7, Table 3). It was found that higher selectivity for F-Ac-F could be produced without NaCl. Increasing the molar ratio of NaOH to furfural not only improves the total condensate yields, but also increases the selectivity for F-Ac-F. Runs 4, 6 and 8 show the effect of NaOH/furfural molar ratio on the product selectivity without adding NaCl. The results show that the selectivity for F-Ac-F gradually increases from 61.8% to 92.2% as the NaOH/furfural ratio increases from 0.13% to 0.48%. Further optimization of the reaction shows that a selectivity of 96.2% for F-Ac-F and 0.002% for F-Ac are achieved in a 200 ml reactor from the aldol condensation of 36.8 wt% furfural in THF with acetone (Run 9, Table 3), in which the mass ratio of organic to aqueous phase is 5.1 : 1 and the NaOH/furfural ratio is 0.37 : 1. This suggests that both the organic-to-aqueous mass ratio and the NaOH/furfural molar ratio have important influence on the selectivity and distribution of final aldol adducts. Scale-up reactions were performed in a 500 ml reactor using the same reaction conditions as that in Run 9 with reaction yields of 90.9% for F-Ac-F and 0.04% for F-Ac, respectively (Run 10, Table 3). Controlling the reaction conditions in the aldol condensation step can be used to tune the ultimate desired composition of C_8 or C_{13} alkanes.

To summarize, the optimized reaction system not only allows the production of targeted F-Ac-F at high yields by using a higher concentration of furfural as the feed, lower amounts of NaOH, and lower amounts of the aqueous phase than those previously reported by Dumesic and co-workers,[34] but also eliminates the use of NaCl, thereby reducing the product cost.

Fig. 2 shows the disappearance of furfural and the selectivity for F-Ac and F-Ac-F as a function of time for Run 1. The conversion of furfural and acetone (not shown here) was almost complete at 35 min after starting the reaction. The selectivity for F-Ac decreases from 11.3% to 3.5% as time increases from 35 min to 20 h, while the selectivity for F-Ac-F gradually increases with time from 42.7% to a final 93.5%, suggesting other reactions are involved besides the aldol condensation of furfural with acetone. In the HPLC chromatogram, an unidentified peak in between F-Ac and F-Ac-F is always present for all reaction conditions starting from the first minutes of the synthesis. This peak gradually decreases as time increases, suggesting that the intermediate products such as β-hydroxy carbonyl compounds are formed during the aldol condensation reaction. In the HPLC chromatograms, the intermediate product has a retention time inbetween that of F-Ac and F-Ac-F, and there are no other products observed from either HPLC or GC–MS. This suggests that the decomposition of the intermediate product to F-Ac-F (and not other products) is the most probable route, in agreement with the previous report by Fakhfakh *et al.*[33]

3.3 Low-temperature hydrogenation

The F-Ac-F dimer in THF produced from the aldol condensation was subsequently hydro-treated in a batch reactor to saturate the three kinds of double bonds (alkene C═C, furan C═C and ketone C═O bonds). Fig. 3 illustrates the influence of reaction temperature and mass of catalyst on the conversion of F-Ac-F. The results show that the hydrogenation rate increases with temperature. For example, F-Ac-F was 91% converted in 25 min at 125 °C, compared with 81.4% conversion in 32 min at 110 °C. In addition, the use of high mass ratio of Ru/C to F-Ac-F can speed up the conversion of F-Ac-F.

The hydrogenation product consists of a mixture of hydrogenated dimers with different degrees of hydrogenation, indicating there exists a multi-step hydrogenation of double bonds of F-Ac-F. Three hydrogenated products were identified during hydrogenation reactions – the spiro, ketone and alcohol form of the dimer, as shown in Fig. 4. The C═C double bonds in the side chain are hydrogenated first to form the intermediate furan ketone, followed by three pathways to form the spiro, ketone and alcohol H-dimers as suggested by Matyakubov *et al.*[40] The intermediate furan ketone and intermediate furan alcohol were not observed in the present study, most likely because these compounds were immediately consumed.[40] The spiro and alcohol H-dimers are fully hydrogenated, and the ketone H-dimer contains only one saturated carbonyl bond.

Fig. 5 shows the F-Ac-F disappearance and selectivity for hydrogenated dimers as a function of time for a typical hydrogenation run over Ru/C at 110 °C and 800 psig. As we can

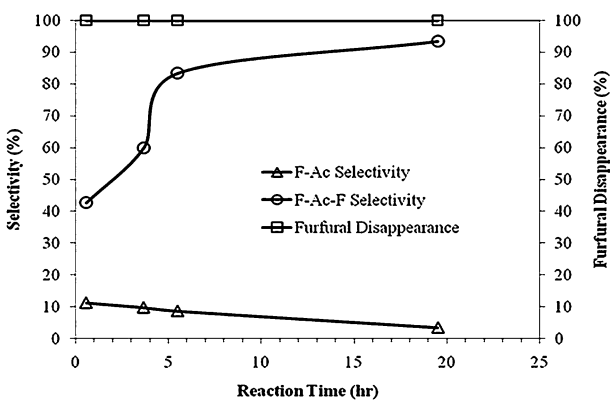

Fig. 2 Furfural disappearance and selectivity for monomer (F-Ac) and dimer (F-Ac-F) as a function of time. The experiment was conducted in a 50 ml batch reactor at 25 °C and atmospheric pressure. The feed concentration of furfural in THF was 13 wt% and NaCl was added to saturate the reactive aqueous phase. Molar ratio of NaOH to furfural = 2.3, mass ratio of organic to aqueous phase = 1.

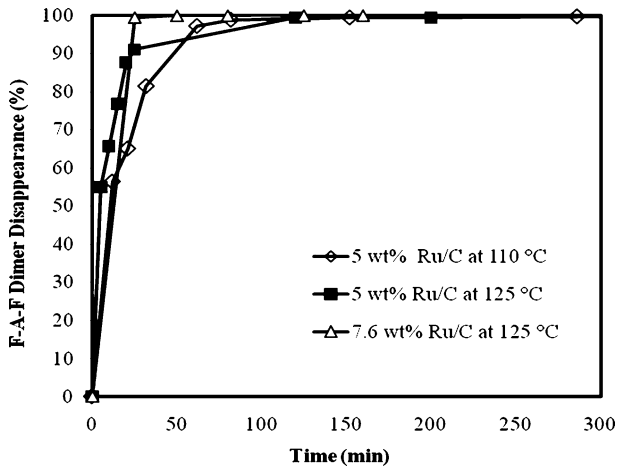

Fig. 3 Hydrogenation of F-Ac-F dimer as a function of time and catalyst concentration. The reactions were conducted in a batch reactor at 800 psig and various temperatures. The feed concentration was 11.5 wt% dimer in THF.

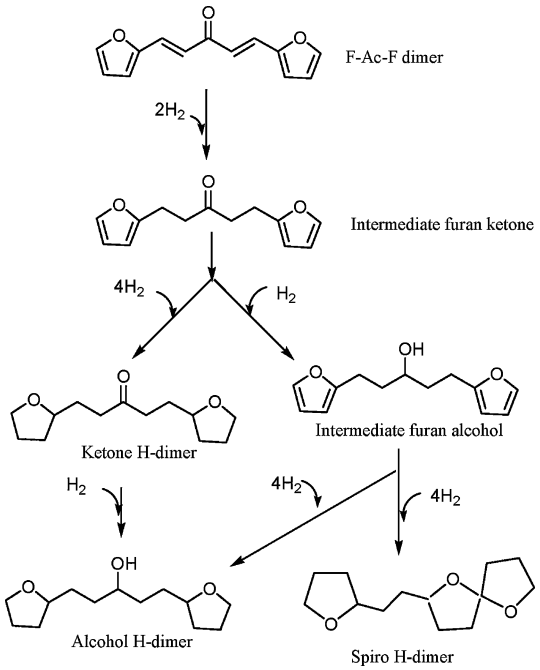

Fig. 4 Reaction pathways for hydrogenation of F-Ac-F dimer to hydrogenated H-dimers at 110 °C and 800 psig with a 5 wt% Ru/C powder catalyst.

see, three types of hydrogenated dimers could be identified within 10 min from starting the reaction. The selectivity of ketone H-dimer quickly reaches a maximum, followed by a continuous decrease to zero concentration at 120 min. The selectivity of spiro H-dimer gradually increases as time increases, and reaches a maximum at 120 min, followed by a slight decrease with time. The selectivity of alcohol H-dimer shows a continuous increase as time increases. The final products, consisting of mainly spiro and alcohol dimers were used to make alkanes in the next step.

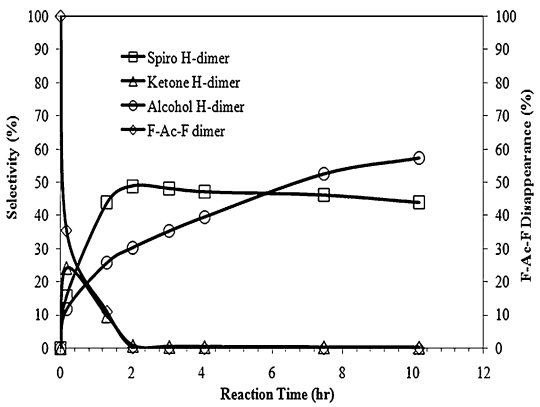

Fig. 5 F-Ac-F disappearance and selectivity for spiro H-dimer, ketone H-dimer, and alcohol H-dimer as a function of time. The reaction was conducted at 110 °C and 800 psig with a 5 wt% Ru/C catalyst. The feed solution contains 11.5 wt% F-Ac-F dimer in THF.

3.4 Hydrodeoxygenation

After low-temperature hydrogenation, the effluent containing mixed hydrogenated dimers and THF was sent to a continuous plug flow bed reactor to make alkanes at 260 °C and 900 psig with a 4 wt% Pt/SiO_2–Al_2O_3 catalyst. Fig. 6 shows the n-alkane distributions from hydrodeoxygenation of H-dimers at a LHSV‡ of 1.1 h^{-1}. The total carbon yield for jet and diesel fuel range alkanes (C_8–C_{13}) was 91%, with tridecane and dodecane being the primary products, each of which accounts for 72.6% and 15.6%, respectively. Based on GC–MS data, the liquid phase also contains very small amounts of two other alkanes larger than C_{13}, *viz.*, 6,9-dimethyltetradecane and 2,6-dimethyldodecane. The H-dimer conversion was 100% under the current conditions, and the Pt/SiO_2–Al_2O_3 did not undergo deactivation even after 120 h testing. In the effluent gas phase, only C_1–C_6 alkanes were observed, and no CO or CO_2 was detected in the products. In the liquid phase, other than THF and alkanes, there were some other organic oxygenates identified by GC–MS, including butanol, butyl propyl ether, butanoic acid, and furan and its derivatives, which are most likely byproducts from THF.

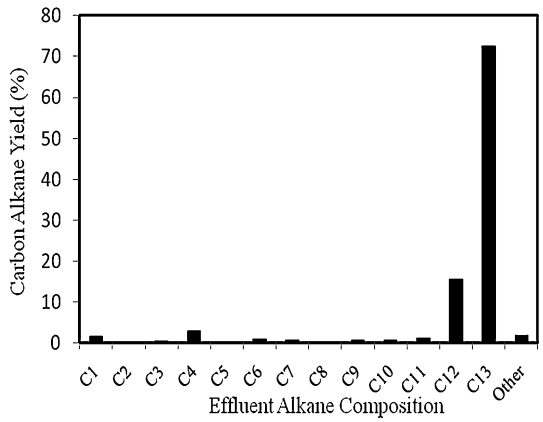

Fig. 6 Carbon alkane yields for the hydrodeoxygenation of H-FAF at 260 °C and 900 psig with a 4 wt% Pt/SiO_2–Al_2O_3 catalyst using a LHSV‡ of 1.1 h^{-1}. The feed contains 7 wt% hydrogenated dimers.

Fig. 7 shows the effect of space velocity on the carbon n-alkane (C_{11}–C_{13}) yields for hydrodeoxygeantion of H-dimers. At a LHSV of 1.1 h^{-1}, all alkane yields reach their maximum values. Increasing the LHSV from 1.1 h^{-1} to 2.5 h^{-1} decreases the tridecane yield from 76.2% to 28.9% due to the low conversion of H-dimers.

4. Discussion

Our experimental results have demonstrated the technological feasibility of obtaining high yields of jet and diesel fuel range alkanes from hemicellulose-derived aqueous solutions. Table 4 lists the current experimental and future target yields for each step for this process. The overall experimentally obtained yield of 76% for jet fuel range alkanes corresponds to a weight-percent yield of 0.46 kg of alkanes per kg of xylose (monomer and oligomers) in the hemicellulose extract. The theoretical yield for this process is 0.61 kg of alkanes per kg of xylose (monomer and oligomers) in the hemicellulose extract. Currently, the low-yielding steps are dehydration and hydrodeoxygenation. For

‡ LHSV is defined as the volumetric flow rate of feed solution divided by the volume of catalyst.

Table 4 Current yields and future target yields for the production of jet and diesel fuel range alkanes from the hemicellulose extract

	Yield (%)				
	Dehydration[a]	Aldol condensation	Hydrogenation	Hydrodeoxygenation	Overall
Current	87	96	100	91	76
Future	95	98	100	95	88

[a] The furfural yield of 81% is used in the case of $M_{org.}/M_{aq.} = 1$ for economic analysis.

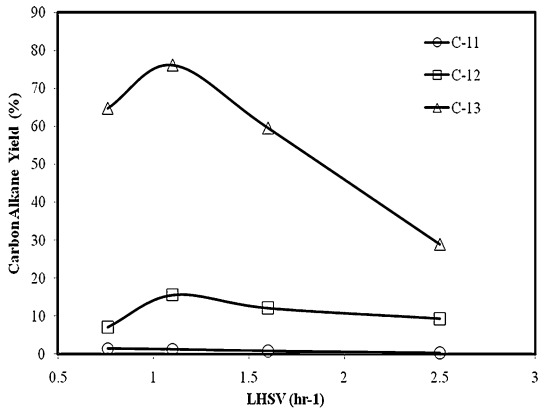

Fig. 7 Effect of LHSV on alkane (C_{11}–C_{13}) yields for hydrodeoxygenation of H-FAF (spiro dimer and alcohol dimer). The reactions were conducted in a continuous plug flow reactor over Pt/SiO_2–Al_2O_3 at 260 °C and 900 psi. The feed contains 5–15 wt% hydrogenated dimer and was prepared by hydrogenation of F-Ac-F dimer in THF at 110 °C and 800 psig for 600 min with a 5 wt% Ru/C catalyst.

the dehydration step, we have been able to obtain a yield of 90% with model xylose solutions, as shown in Table 2. The kinetic model for the dehydration of xylose in a biphasic reactor suggests that a yield of 95% can be achieved with MIBK–water as solvent at elevated temperatures and shorter residence time.[41] Therefore it should be possible to obtain yields close to 95% for this process by further optimizing the reaction system. Yields higher than 95% are very challenging due to the undesired decomposition and polymerization reactions. The yield for the hydrodeoxygenation step could also be improved from 91% to 95% with improvements in the catalysts and reactor design. We predict that the overall yield for jet and diesel fuel range alkanes could be increased up to 88% (as shown in Table 4) with these modest process improvements. The straight alkanes produced in our process can be further upgraded *via* the hydroisomerization process to form branched alkanes. The straight and branched alkanes together can either be directly sold as chemicals or liquid fuels, or sent to a refinery as additives to make the desired jet and diesel fuels by blending with other hydrocarbons. Currently the alternative approach to the synthesis of straight and branched alkanes for synthetic jet and diesel fuels is the Fischer–Tropsch process, using synthesis gas derived from natural gas.[42] As such, our process provides another way to make jet and diesel fuels range alkanes from waste hemicellulose-derived solutions. Next we will show how our four-step process can be integrated for a production plant, and a preliminary economic analysis for our process is performed to evaluate the product cost.

4.1 Integrated process flow and materials balance

Fig. 8 shows a process flow diagram and Table S2† shows the material balances for making jet and diesel fuel range alkanes from hemicellulose extracts. The material balance in Table S2

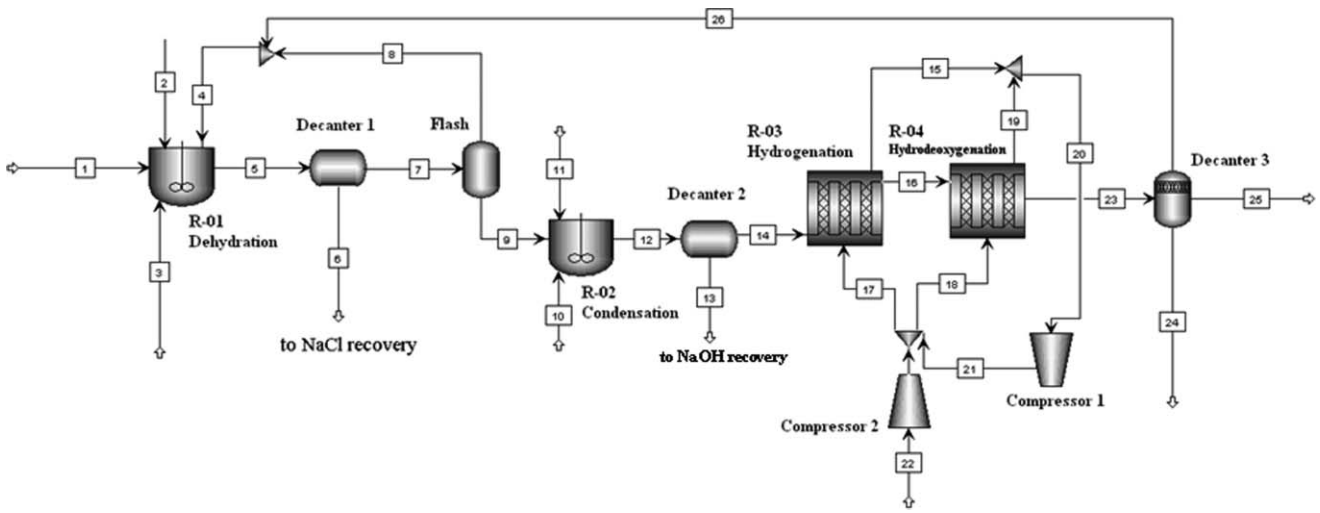

Fig. 8 Process flow diagram for the production of jet fuel range alkanes from hemicellulose-derived aqueous solutions. Process stream key: 1. 3.3 wt% hemicellulose extract; 2. NaCl; 3. 37 wt% HCl; 4. THF; 5. Furfural + THF + aq. phase; 6. Aq. phase, 7. Furfural + THF; 8. THF; 9. Furfural + THF; 10. Acetone; 11. 26 wt% NaOH; 12. F-Ac-F + THF + aq. phase; 13. Aq. phase; 14. F-Ac-F + THF; 15,19,20,21. Recycling streams of H_2; 16. H-FAF; 17,18. Input H_2; 22. Fresh charge of H_2; 23. Tridecane + THF + aq. phase; 24. Aq. phase; 25. Tridecane; 26. THF.

assumes a 100% yield for each step. The hemicellulose extract (Stream 1), solid NaCl (Stream 2), concentrated 37 wt% HCl solution (Stream 3) and the NaCl-pretreated THF (Stream 4) are co-fed to the first biphasic reactor (R-01) which is assumed to be a CSTR-type reactor. Equal weights of organic and aqueous phase are used here. The NaCl content relative to the sugar solution is 20 wt% as shown in Table S2. In this reactor, furfural is produced *via* the biphasic dehydration of xylose at 160 °C and 220 psig with a residence time of 5 min. These reaction conditions were obtained from our experimental results as shown in Table 2. The reactor effluent (Stream 5) is then sent to Decanter 1 where THF and furfural (Stream 7) are separated from the aqueous phase (Stream 6). The aqueous phase could be further processed to recover NaCl, HCl, lactic acid, formic acid and acetic acid.[8,13,51] After a liquid–liquid split, the organic phase (Stream 7) is sent to the 'Flash' to concentrate furfural to 37 wt% (Stream 9) by removing the majority (96%) of THF. The removed THF (Stream 8) is recycled back to the first reactor (R-01). The concentrated furfural in THF (Stream 9), 26 wt% NaOH solution (Stream 11) and acetone (Stream 10) are co-fed into the second well-mixed reactor (R-02), where the F-Ac-F dimer is produced *via* the aldol condensation at room temperature and atmospheric pressure for a residence time of 24 h. These are the same reaction conditions used for the aldol condensation as shown in Table 3 This reactor effluent contains mainly the organic phase (THF and F-Ac-F dimer produced) and a small amount of aqueous phase. The aqueous phase (Stream 13) is removed *via* Decanter 2 and could be further processed to recover NaOH, and the organic phase (Stream 14) together with H_2 (Stream 17) are fed to the hydrogenation reactor (R-03) where the F-Ac-F dimer is hydrogenated to form H-FAF at 110 °C and 800 psig with a 5 wt% Ru/C catalyst as described in Section 2.2. The H-FAF in THF (Stream 16) together with H_2 (Stream 18) are finally fed to the hydrodeoxygenation reactor (R-04) where the production of jet and diesel fuel range alkanes take place at 260 °C and 900 psig with a 4 wt% Pt/Al_2O_3-SiO_2 catalyst. In the last two steps, H_2 is fed by using compressors (Compressor 1 and Compressor 2) and a ratio of excess H_2 to fresh-charging H_2 of 2 is used. The effluent from the hydrodeoxygenation reactor (Stream 23) is sent to Decanter 3 where the remaining THF is vaporized and recycled back to R-01 (Stream 26), water (Stream 24) is removed *via* a liquid–liquid split, and jet and diesel fuel range alkanes (Stream 25) are obtained from the organic phase. For all decanters, the projected temperature and pressure are 25 °C and 14.7 psia.

4.2 Preliminary economic analysis

4.2.1 Raw materials cost. The raw materials cost is calculated based on the current yields and future target yields as shown in Table 4. Preliminary analysis by researchers at the Univeristy of Maine shows that the estimated cost of xylose derived from pre-processing extracts at an integrated forest products refinery co-located at a hardwood Kraft mill or biomass boiler is on the order of $0.15/kg on a dry basis. This cost accounts for sugar heating value lost by the host mill, the costs of extracting and concentrating the extract, and the costs and revenue associated with recovering acetic acid as a co-product. In our calculations the price of $0.1/kg dry xylose is used as the base case. H_2 is employed from an external source and its purchase price can vary significantly depending on the location of a new plant to be built. The price of H_2 considered in our calculation is based on a report released by the National Renewable Energy Laboratory.[44] Assuming that the new plant is built in a place close to a H_2 production plant, the H_2 price can be as low as $1.0/kg. The acetone at the time of this analysis is available for $0.7/kg. As a result, for the base case the overall raw materials cost is $1.79/gal and $1.60/gal jet and diesel fuel range alkanes based on current yields and future target yields, respectively. For the base case, H_2 costs $0.41/gal and $0.39/gal, xylose costs $0.66/gal and $0.53/gal and acetone costs $0.72/gal and $0.68/gal for current yields and future target yields, respectively. The cost of acetone represents approximately 41% of the raw materials cost. It should be noted that for this economic analysis we are not including the cost of NaCl or any disposal costs; the NaCl is considered to be recycled in our process.

4.2.2 Installed equipment cost and associated utility cost. Table 5 shows a summary of installed equipment cost and associated utility cost for three different plant capacities based on the current yields and future target yields. The cost for installed equipment and associated utility are calculated based on the cost correlations described by J. M. Douglas.[43] Some equipment, such as pumps and heat exchangers, are not included and will be added in our future detailed analysis when more detailed information is available. The installed equipment cost for all reactors also includes the catalyst cost. The costs of Ru and Pt we used in R-03 and R-04 are estimated from the online market value.[45–46] It should be noted that the costs for HCl and NaOH we used in R-01 and R-02 are not included for this economic analysis. The total installed equipment cost is M$1.11, M$5.61 and M$44.30 for 0.5 Mgal/yr, 5 Mgal/yr and 50 Mgal/yr plant capacities based on current yields, respectively. The total equipment cost can be reduced by 8.2%, 10.3% and 15.0% for 0.5 Mgal/yr, 5 Mgal/yr and 50 Mgal/yr plant capacities based on the future target yields, respectively. The most expensive piece of equipment in this process is the cost of the reactor for the aldol condensation step, which accounts for roughly 50% of the equipment cost. This high cost is due to the long residence time in this reactor. This suggests the cost could be reduced by operating at a lower residence time.

The utility cost consists of the electricity cost for compressors and the steam cost for R-01, Flash and Decanter 3. Basic heat integration is applied for R-01, Flash and a possible Decanter 3. Heat released by cooling the output stream of R-01 can be used to supply the energy required for the Flash and a possible Decanter 3.

The latent heat of THF vapor streams from Flash and Decanter 3 can be used to preheat the input xylose solution of R-01. We may also need heating supplies for R-03 and R-04; however, for this economic analysis we are ignoring these costs. These costs are most likely small because of the low flows, the low concentration of water and the fact that no phase change is occurring in the reactor.

As shown in Table 5, the total utility costs increase linearly from M$0.39 to M$3.85 to M$38.52 when the plant capacity increases from 0.5 Mgal/yr to 5 Mgal/yr to 50 Mgal/yr. The

Table 5 Summary of equipment and utility costs of different process scales calculated based on the current yield (outside the parenthesis) and future yield targets (inside the parenthesis), respectively (4th quarter 2007)

	0.5 (Mgal/yr)		5 (Mgal/yr)		50 (Mgal/yr)	
Equipment	Installation cost (k$)[a]	Associated utility cost (k$/yr)	Installation cost (k$)[a]	Associated utility cost (k$/yr)	Installation Cost (k$)[a]	Associated utility cost (k$/yr)
R-01 [b]	134 (134)	377 (295)	490 (416)	3767 (2947)	2543 (2311)	37 675 (29 470)
R-02	509 (432)		2668 (2422)		24 012 (20 010)	
R-03	87 (80)		595 (526)		5047 (4359)	
R-04	87 (80)		601 (531)		5106 (4414)	
Decanter 1	75 (75)		318 (274)		1937 (1422)	
Decanter 2	10 (10)		53 (35)		160 (160)	
Decanter 3 [c]	5 (5)	Integrated	19 (19)	Integrated	87 (70)	Integrated
Flash [c]	53 (53)	Integrated	195 (160)	Integrated	1049 (711)	Integrated
Compressor 1 [d]	54 (54)	1 (1)	96 (96)	7 (7)	559 (538)	74 (71)
Compressor 2 [d,e]	96 (96)	8 (7)	580 (554)	77 (73)	3798 (3657)	766 (734)
Total	1110 (1019)	386 (303)	5614 (5033)	3851 (3027)	44 298 (37 651)	38 515 (30 275)

[a] The costs for installed equipment and associated utility are calculated based on the cost correlations described by J. M. Douglas.[43] [b] Assuming (1) the temperature of the feed sugar solution is 25 °C, (2) the heat released by condensing THF vapor stream is recycled back to pre-heat the sugar solution, (3) the temperature of recycled THF is 65 °C, and (4) the cost of a 120 psig steam is 4.4 US$ per 1000 lb. [c] Heating energy is supplied by the heat released from cooling the output stream of R-01. [d] Assuming (1) the pressure drop across the reactors is 30 psi, (2) excess H_2 is twice as much as the stoichiometric amount, (2) process operation time as 8150 h/yr and (3) electricity cost is 0.064 $/kWh (US national average electricity price for industry section in 2007). [e] Assuming that H_2 comes out of the pipeline with a pressure of 340 psi.[44]

total utility costs can be reduced by 21.5% for all three capacities if the yield improves to the future target yields. Among the utility costs, it is interesting to note that R-01 accounts for about 98% of total utility cost for all three plant capacities due to the low concentration of sugar solution treated in R-01. As discussed below, the total utility cost can decrease significantly if a high concentration of sugar solution is used as the feed to R-01.

4.2.3 Product cost. Based on raw materials cost, utility cost and installed equipment cost, we calculated the total annual product cost using the following equation:[43]

Total annual product cost ($/yr) = 1.031 (raw materials cost + utility cost) + 0.186 (installed equipment cost) + 2.13 (labor cost) + general expenses

In this equation, it is assumed that general expenses including sale, administration, research and engineering are about 2.5% of total revenue. Fig. 9 shows the calculated unit production cost as a function of production capacity for current yields and future target yields. For the production capacity as low as 0.5 Mgal/yr, the unit production cost is estimated to be $4.39/gal and $4.01/gal for current yields and future target yields, respectively. The unit production cost decreases sharply as production capacity increases up to 5 Mgal/yr ($3.17/gal and $2.79/gal for current yields and future target yields, respectively). Further increase in the production capacity results in a less dramatic decrease in the unit product cost, which approaches $2.92/gal and $2.54/gal, respectively, as the production capacity approaches 50 Mgal/yr.

The contribution (%) of the raw materials cost in the final product cost increases from 44.6% to 63.0% as production capacity increases from 0.5 Mgal/yr to 50 Mgal/yr.

4.2.4 Sensitivity analysis. A sensitivity analysis was performed to help identify how cost could be decreased in the future, and where to focus future research efforts. The cost of the raw materials is a significant part of the cost, and finding

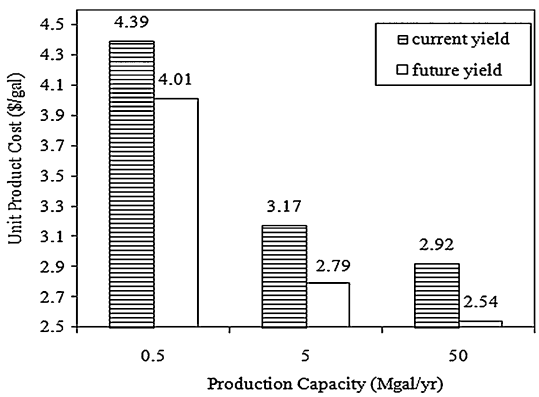

Fig. 9 Unit production cost as a function of production capacity based on the current and future target yields. We assume that (1) the price for xylose, acetone and H_2 is $0.1/kg, $0.7/kg, and $1.0/kg, respectively, (2) there are three shifts with all processes, 1 operator per shift, 2 operators per shift and 4 operators per shift for the process with 0.5, 5 and 50 Mgal/yr, respectively. Labor cost = 10^5 $/operator, and (3) in the revenue calculation, the selling price of product is $3/gal.

a cheaper source of raw materials can significantly reduce the product cost. Table 6 summarizes the sensitivity analysis of raw materials cost. As the xylose price doubles, the raw materials cost will increase by 36.9% and by 33.1% for current yields and future target yields, respectively. As the price of H_2 doubles, the raw materials cost will increase by 22.9% and by 24.4% for the current yields and future target yields, respectively. Compared to H_2 and xylose, the acetone price has the most significant impact on raw materials cost. As the acetone cost doubles, the raw materials cost increases by 40.2% and 42.5% based on current yields and future target of yields, respectively.

The majority of the utility cost is associated with the heat required for R-01 which is used to heat the sugar solution and THF to the reaction temperature of 160 °C as shown in Table 5. If the feed xylose concentration in the hemicellulose

Table 6 Sensitivity analysis of raw materials cost on prices of xylose, H_2 and acetone. The italicised data refer to the cost for the base case

Feedstocks	Price ($/kg)	Raw Materials Cost w/ Current Yield ($/gal)	Raw Materials Cost w/ Future Yield target ($/gal)
Xylose[a]	0.20	2.45	2.13
	0.15	2.12	1.86
	0.10	*1.79*	*1.60*
H_2[b]	2.0	2.20	1.99
	1.5	2.00	1.80
	1.0	*1.79*	*1.60*
Acetone[c]	1.4	2.51	2.28
	1.05	2.15	1.94
	0.7	*1.79*	*1.60*

[a] With acetone prices as $0.7/kg, H_2 price as $1.0/kg. [b] With acetone price as $0.7/kg, xylose price as $0.1/kg. [c] With H_2 price as $1/kg, xylose price as $0.1/kg.

extract increases, the heating requirement for R-01 decreases, consequently leading to the decrease of the utility cost for R-01. The sizes of R-01 and Decanter 1 also decrease with increasing xylose concentration, leading to a lower installed equipment cost.

Therefore, increasing the xylose concentration in the hemicellulose extract can significantly decrease both the installed instrument cost and the utility cost as shown in Table 7. As the xylose concentration increases from 3 wt% to 10 wt%, the installed cost and utility cost decrease by 39.5% and by 68.1%, respectively, for a plant capacity of 50 Mgal/yr. Fig. 10 shows the unit product cost as a function of both the production capacity and the xylose concentration in the hemicellulose extract assuming the future yield scenario. Increasing the feed xylose concentration can significantly decrease the unit product cost. Compared to the 3 wt% xylose case, the unit product cost for 10 wt% xylose case can further decrease by 18.9% from $2.54/gal to $2.06/gal for the production capacity of 50 Mgal/yr. The price of $2.06/gal is actually lower than the current US market jet fuel price.[47]

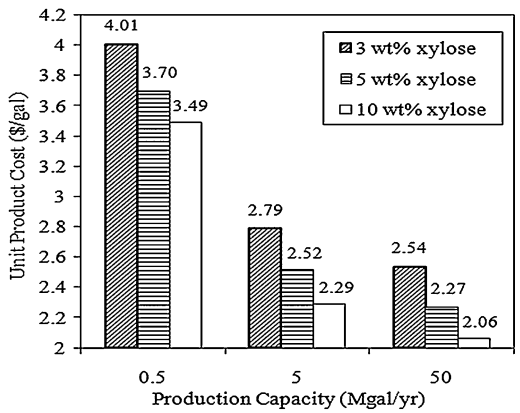

Fig. 10 The total product cost varies as a function of production capacity and feed xylose concentration based on the future yields. The assumptions are the same as those in Fig. 9.

Modifying the organic-to-aqueous mass ratio in R-01 does not significantly change the product cost, as shown in Fig. 11. This analysis was performed based on current yields assuming that the 3 wt% xylose in the hemicellulose extract is used as the feed. At the mass ratio of 1, all unit product costs reach their minimum values. Increasing the organic-to-aqueous mass ratio from 1 to 2 is favorable to increase the yield of furfural (from 81% to 87%), but causes the unit product cost to increase due to increased installed and utility costs. Decreasing the mass ratio to 0.67 also increases the unit product cost resulting from the significant drop of furfural yield (from 81% to 62%). The mass ratio of 1 should be used in order to minimize the product cost.

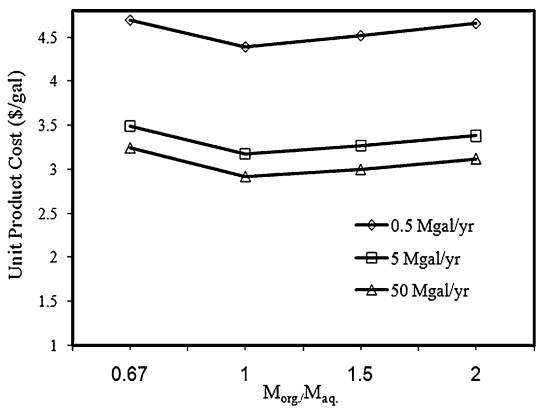

Fig. 11 Effect of the organic-to-aqueous mass ratio ($M_{org.}/M_{aq.}$) in the biphasic dehydration step on the unit product cost at different production capacities. The data were calculated based on the current yields assuming the xylose concentration in the hemicellulose extract is 3 wt%.

A sensitivity analysis of the Pt and Ru catalyst cost for R-03 and R-04 on the unit product cost was also conducted. This result suggests that the contribution of the catalyst cost to the unit product cost is below 1% for all cases, suggesting that the catalyst cost of Ru and Pt is not a major factor affecting product cost.

These results here suggest that the most important variable affecting product costs is the cost of the raw materials. Finding cheap raw material is the top priority in making this process commercial. Currently acetone is used as a coupling agent, but in the future methods to form C–C bonds directly from furfural-derived molecules can be developed.[48–49] The second most important variable affecting the product cost is finding high concentrations of sugar solutions, as this significantly affects the product cost. We should note here that the sugar streams used in our process are derived from wood-processing industries

Table 7 Sensitivity analysis of the xylose concentration in the hemicellulose extract on the equipment cost and utility cost, with future target yields [a] (4th quarter 2007)

	3 wt% xylose		5 wt% xylose		10 wt% xylose	
Process scale (MG/yr)	Installation cost (k$)	Utility cost (K$/yr)	Installation cost (k$)	Utility cost (k$/yr)	Installation cost (k$)	Utility cost (k$/yr)
0.5	1019	303	849	185	769	96
5	5033	3027	4192	1849	3097	965
50	37 651	30 275	29 621	18 487	22 795	9646

[a] Using the same assumption as Table 5.

that do not derive high value from hemicelluloses, typically burning it for energy. Thus, hemicellulose extracts derived from established wood-processing industries hold promise to be some of the cheapest streams available. Improving the yield of the process steps could also decrease the product cost by 13% for the production capacity of 50 Mgal/yr. Yields can be improved by using better catalysts and designing more efficient reactors. Most of the reactions reported in this process have not been studied in any great detail. In our economic analysis we are neglecting the costs of HCl and NaOH. The cost of NaOH was negligible compared to the costs of Ru and Pt, and NaOH can be easily recovered due to its high concentrations in the aqueous phase obtained from the aldol condensation. However, the cost of HCl can significantly affect the unit product cost depending on the feed xylose concentration in the hemicellulose extract. For example, based on future target yields, the unit product cost can increase by 12.5% for 3 wt% xylose concentration and by 4.4% for 10 wt% xylose concentration as the feeds, respectively, for the production capacity of 5 Mgal/yr. Therefore, recycling the HCl or switching to solid acids would be helpful to minimize the costs for this process.

4.2.5 Integration with other processes. Our four-step process obtaining jet and diesel fuel range alkanes from hemicellulose-derived aqueous solutions can be integrated into a biomass boiler operation, a pulp and paper refinery or into a lignocellulosic ethanol refinery. Fig. 12 shows the integrated conceptual lignocellulosic biomass refinery for the production of renewable chemicals and liquid fuels. The lignocellulosic biomass is first treated with either a dilute acid or a hot water steam to release hemicellulose extract. The hemicellulose extract is processed to make either jet and diesel fuel range alkanes (C_8–C_{13}) with our process, or ethanol and acetic acid by using the "near-neutral" hemicellulose pre-extraction process.[13,49] The C_6 aqueous portion can also be used as a feedstock to make jet and diesel fuel range alkanes as shown in Fig. 12. The aqueous products obtained from biphasic dehydration are either fed to the pre-extraction process for recovery of acetic acid or recycled back to the hydrolysis process if the acid hydrolysis is used. The cellulose fraction in the residual solids is either sent to a conventional Kraft pulping process[13,49] or hydrolyzed with an acid or enzyme to release cellulose-derived sugar solution containing mainly glucose. The derived sugar solution is processed to make either

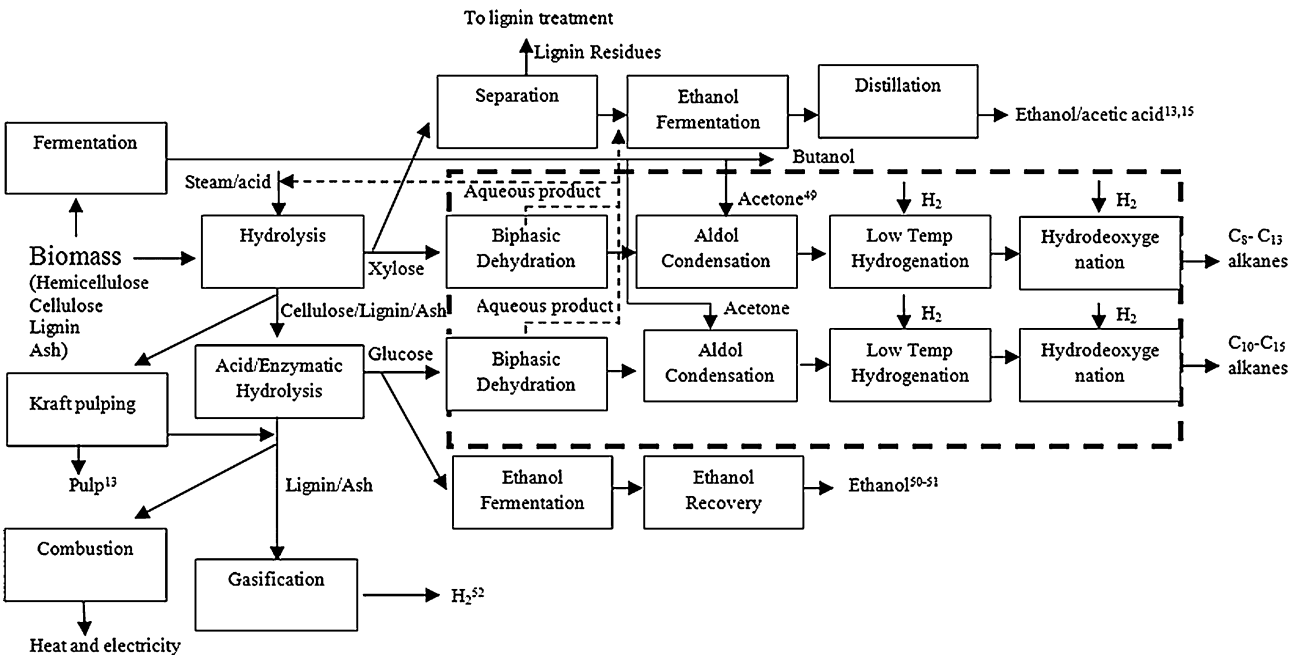

Fig. 12 Integrated conceptual lignocellulosic biorefinery for the production of renewable chemicals and liquid fuels. The four-step process to make straight-chain alkanes is marked with a bold dashed line.

jet and diesel fuel range alkanes (C_{10}–C_{15}) with our process or bioethanol through commercialized fermentation processes.[50–51] The residual lignin fraction, separated from either Kraft pulping process or the acid/enzymatic hydrolysis, is either burned to provide the heat and electricity needed to run our process or treated through gasification to make H_2, as a supply for the use in low-temperature hydrogenation and high-temperature hydrodeoxygenation units in our process.[52] Acetone used in the aldol condensation unit can be supplied by the fermentation of biomass.[53] All raw materials required in our process can be internally supplied through the integrated processes, as a way of reducing the product cost.

5. Conclusions

Jet and diesel fuel range alkanes (C_8–C_{13}) can be produced from waste hemicellulose-derived aqueous solutions by using a four-step integrated process that includes: (1) acid hydrolysis and xylose dehydration, (2) aldol condensation, (3) low-temperature hydrogenation, and (4) high-temperature hydrodeoxygenation. The first step in this process is the combined acid hydrolysis of xylose oligomers into xylose followed by the acid-catalyzed biphasic dehydration of xylose into furfural. The furfural extract from the aqueous phase is then sent to an aldol condensation unit where the alkane precursor F-Ac-F is formed through the reaction of furfural with acetone (furfural/acetone molar ratio = 2). The F-Ac-F dimer in the organic phase is then sent to a low-temperature hydrogenation unit where thermally unstable F-Ac-F is hydrogenated to thermal stable hydrogenated dimers (H-FAFs). In this step, three types of double bonds of F-Ac-F are saturated and the final hydrogenated dimers contain mainly spiro and alcohol forms of dimers. Finally, the hydrogenated dimer solution and H_2 are co-fed to the hydrodeoxygenation unit to produce jet and diesel fuel range alkanes over a bifunctional catalyst. Under optimized conditions, the yield for alkanes (C_8–C_{13}) is 91%, with tridecane and dodecane being the primary products with carbon selectivities of 72.6% and 15.6%, respectively. The theoretical yield for this process is 0.61 kg of jet fuel per kg of xylose (monomer or oligomers) in the hemicellulose extract. Experimentally, we are able to produce 0.46 kg of jet fuel per kg of xylose in the hemicellulose extract, which is 76% of the theoretical yields.

Preliminary economic analysis for this process was performed based on the simplified process flow diagram and material balances with the consideration of two scenarios, current yields and future target yields. We calculate the installed equipment cost, the associated utility cost and the total product cost as a function of production capacities. We estimate that jet and diesel fuel range alkanes can be produced from between $2.06/gal to $4.39/gal depending on the feed xylose concentration in the hemicellulose extract, the size of the plant capacity and the overall yields. Sensitivity analysis shows that the prices of raw materials, the organic-to-aqueous mass ratio in the biphasic dehydration step and the feed xylose concentration in the hemicellulose extract significantly affect the product cost.

Acknowledgements

This work was supported by the Defense Advanced Research Project Agency through the Strategic Technology Office (BAA 08-07) (Approved for Public Release, Distribution Unlimited). The views, opinions, and/or findings contained in this article/presentation are those of the author/presenter and should not be interpreted as representing the official views or policies, either expressed or implied, of the Defense Advanced Research Projects Agency or the Department of Defense. The authors wish to express their gratitude to Prof. Michael F. Malone at the University of Massachusetts for helpful discussions, Justin Crouse and Dr Martin Lawoko at the University of Maine for sending sugar solutions for this study, and Dr Dora Lopez de Alonzo at Logos Technologies for helpful discussions.

References

1 Y. Roman-Leshkov, C. J. Barrett, Z. Y. Liu and J. A. Dumesic, *Nature*, 2007, **447**, 982–985.
2 G. W. Huber, S. Iborra and A. Corma, *Chem. Rev.*, 2006, **106**, 4044–4098.
3 R. E. H. Sims, W. Mabee, J. N. Saddler and M. Taylor, *Bioresour. Technol.*, 2010, **101**, 1570–1580.
4 G. W. Huber and J. A. Dumesic, *Catal. Today*, 2006, **111**, 119–132.
5 T. P. Vispute and G. W. Huber, *Green Chem.*, 2009, **11**, 1433–1445.
6 S. Czernik, R. French, C. Feik and E. Chornet, *Ind. Eng. Chem. Res.*, 2002, **41**, 4209–4215.
7 F. Carrasco, *Wood Fiber Sci.*, 1993, **25**, 91–102.
8 G. Vially, R. Marchal and N. Guilbert, *World J. Microbiol. Biotechnol.*, 2009, **26**, 307–614.
9 D. C. Elliott, D. Beckman, A. V. Bridgwater, J. P. Diebold, S. B. Gevert and Y. Solantausta, *Energy Fuels*, 1991, **5**, 399–410.
10 T. R. Carlson, G. A. Tompsett, W. C. Conner and G. W. Huber, *Top. Catal.*, 2009, **52**, 241–252.
11 P. B. Weisz, W. O. Haag and P. G. Rodewald, *Science*, 1979, **206**, 57–58.
12 M. H. Thomsen, A. Thygesen, H. Jorgensen, J. Larsen, B. H. Christensen and A. B. Thomsen, *Appl. Biochem. Biotechnol.*, 2006, **130**, 448–460.
13 H. Mao, J. M. Genco, S. H. Yoon, A. van Heiningen and H. Pendse, *J. Biobased Mater. Bioenergy*, 2008, **2**, 177–185.
14 L. R. Lynd, R. T. Elander and C. E. Wyman, *Appl. Biochem. Biotechnol.*, 1996, **57–8**, 741–761.
15 H. B. Mao, J. M. Genco, A. van Heiningen and H. Pendse, *Bioresources*, 2010, **5**, 525–544.
16 S. Walton, A. van Heiningen and P. van Walsum, *Bioresour. Technol.*, 2010, **101**, 1935–1940.
17 G. W. Huber, P. O'Connor and A. Corma, *Appl. Catal., A*, 2007, **329**, 120–129.
18 G. W. Huber, R. D. Cortright and J. A. Dumesic, *Angew. Chem., Int. Ed.*, 2004, **43**, 1549–1551.
19 G. Hemighaus, T. Boval, J. Bacha, F. Barnes, M. Franklin, L. Gibbs, N. Hogue, J. Jones, D. Lesnini, J. Lind and J. Morris, *Aviation Fuels Technical Review (FTR-3)*, Chevron Corporation, 2006.
20 H. T. Mayfield, *JP-8 Compositions and Variability, A. L. E. R. Division, Report AL/EQ-TR-1996-0006*, Tyndall Air Force Base, FL, 1996.
21 G. W. Huber, J. N. Chheda, C. J. Barrett and J. A. Dumesic, *Science*, 2005, **308**, 1446–1450.
22 J. N. Chheda, Y. Roman-Leshkov and J. A. Dumesic, *Green Chem.*, 2007, **9**, 342–350.
23 B. H. Um and G. P. van Walsum, *Appl. Biochem. Biotechnol.*, 2010, **161**, 432–447.
24 S. Walton, Ph.D. Thesis, The University of Maine, 2009.
25 L. C. Bryner, L. M. Christensen and E. I. Fulmer, *Ind. Eng. Chem.*, 1936, **28**, 206–208.
26 M. J. Antal, T. Leesomboon, W. S. Mok and G. N. Richards, *Carbohydr. Res.*, 1991, **217**, 71–85.
27 A. S. Dias, M. Pillinger and A. A. Valente, *J. Catal.*, 2005, **229**, 414–423.
28 Y. Roman-Leshkov, J. N. Chheda and J. A. Dumesic, *Science*, 2006, **312**, 1933–1937.
29 C. Moreau, R. Durand, S. Razigade, J. Duhamet, P. Faugeras, P. Rivalier, P. Ros and G. Avignon, *Appl. Catal., A*, 1996, **145**, 211–224.

30 C. Moreau, R. Durand, D. Peyron, J. Duhamet and P. Rivalier, *Ind. Crops Prod.*, 1998, **7**, 95–99.
31 B. Sain, A. Chaudhuri, J. N. Borgohain, B. P. Baruah and J. L. Ghose, *J. Sci. Ind. Res. India*, 1982, **41**, 431–438.
32 D. L. Williams and A. P. Dunlop, *Ind. Eng. Chem.*, 1948, **40**, 239–241.
33 N. Fakhfakh, P. Cognet, M. Cabassud, Y. Lucchese and M. D. D. L. Rios, *Chem. Eng. Process.*, 2008, **47**, 349–362.
34 R. M. West, Z. Y. Liu, M. Peter, C. A. Gartner and J. A. Dumesic, *J. Mol. Catal. A: Chem.*, 2008, **296**, 18–27.
35 J. O. Metzger, *Angew. Chem., Int. Ed.*, 2006, **45**, 696–698.
36 D. A. Isacescu, V. Kenyeres-Ursu, I. Rebedea and F. Tomus, *Analele Universitatii Bucuresti, Seria Stiintele Naturii*, 1965, **14**, 87–93.
37 I. F. Bel'skii and R. A. Karakhanov, *Izvestiya Akademii Nauk SSSR, Seriya Khimicheskaya*, 1962, 905–907.
38 C. R. Russell, H. E. Smith, L. S. Hafner and L. E. Schniepp, *J. Am. Chem. Soc.*, 1953, **75**, 726–727.
39 A. D. Petrov, S. V. Zakharova and V. G. Glukhovtsev, *Dokl. Akad. Nauk SSSR*, 1963, **153**, 1346–1349.
40 R. Matyakubov and Y. M. Mamatov, *Khim. Geterotsiklicheskikh Soedin.*, 1981, 889–893.
41 R. Weingarten, J. Cho, J. W. C. Conner and G. W. Huber, *Green Chem.*, 2010, **12**, 1423–1429.
42 K. Kumar and C. J. Sung, *Fuel*, 2010, **89**, 2853–2863.
43 J. M. Douglas, *Conceptual design of chemical processes*, McGraw-Hill, 1988.
44 M. Ruth, M. Laffen and T. A. Timbario, *Hydrogen pathways: cost, well-to-wheels energy use, and emissions for the current technology status of seven hydrogen production, delivery, and distribution scenarios*, National Renewable Energy Laboratory, Golden, CO, 2009.
45 From http://www.cmegroup.com/trading/metals/.
46 From http://www.platinum.matthey.com/.
47 From http://www.iata.org/whatwedo/economics/fuel_monitor/Pages.
48 V. Nair, K. G. Abhilash and N. Vidya, *Org. Lett.*, 2005, **7**, 5857–5859.
49 A. S. K. Hashmi, M. C. Blanco, E. Kurpejovic, W. Frey and J. W. Bats, *Adv. Synth. Catal.*, 2006, **348**, 792–792.
50 M. Sedlak and N. W. Y. Ho, *Appl. Biochem. Biotechnol.*, 2004, **113–16**, 403–416.
51 C. E. Wyman, *Trends Biotechnol.*, 2007, **25**, 153–157.
52 T. Furusawa, T. Sato, H. Sugito, Y. Miura, Y. Ishiyama, M. Sato, N. Itoh and N. Suzuki, *Int. J. Hydrogen Energy*, 2007, **32**, 699–704.
53 R. Marchal, M. Ropars, J. Pourquié, F. Fayolle and J. P. Vandecasteele, *Bioresour. Technol.*, 1992, **42**, 205–217.

